Interaction Between Superoxide Dismutase and Dipalmitoylphosphotidylglycerol Bilayers: A Fourier Transform Infrared (FT-IR) Spectroscopic Study

Yu-Li Lo[1,2] and Yueh-Erh Rahman[1,3]

Received September 5, 1995; accepted November 9, 1995

Purpose. Superoxide dismutase (SOD), an antioxidant enzyme, converts peroxide radicals into hydrogen peroxide. Liposomes have been used as carriers for SOD to enhance its antioxidant effect. Our previous DSC study has suggested that SOD binding to dipalmitoylphosphatidylglycerol (DPPG) may protect lipid membranes against oxygen-mediated injury. We now present FT-IR studies on the effect of DPPG binding on the temperature-induced SOD folding-unfolding process.

Methods. The FT-IR spectra of SOD in D_2O or DPPG membranes are measured as temperatures increase from 28° to 121°C at a rate of 0.5°C/min. From the quantitative determination of the changes in the amide I band components of the Fourier self-deconvoluted spectra, the DPPG-induced changes of SOD secondary structure could be detected as a function of temperature.

Results. We observe that the relative intensity of the SOD bands from 28°C to 77°C show graduate loss of β-sheet "distorted" structure, loss of turns, and existence of an intermediate state around 50°C. Beginning at 80°C, changes are obtained in three temperature regions: (i) 80°C, (ii) 92°C, (iii) 109°C. The result suggests that SOD folding/unfolding transition involves mostly the relative changes within the regions of helix-like hydrogen bonding pattern, turn, twisted β-bend and irregular structures. When SOD is bound to DPPG, the conformational changes shift to lower temperatures, indicating a reduction of SOD thermal stability. In addition, the gel to liquid crystalline phase transition temperature of DPPG increases from 42°C to 43.5°C.

Conclusions. These results suggest that the thermal stability of SOD is reduced by DPPG binding. However, DPPG bilayer is stabilized by the presence of SOD.

KEY WORDS: superoxide dismutase; lipid membranes; FT-IR; conformation; thermal stability; curve-fitting.

INTRODUCTION

Free radical-mediated injury is the cause of a number of diseases, ranging from arthritis to respiratory distress syndrome, aging and cancer (1). Because of the ubiquity of molecular oxygen (O_2) in aerobic organisms and its ability to accept electrons, oxygen-centered free radicals are often mediators of cellular free radical reactions. Oxygen is also the primary therapeutic agent to treat hypoxemia observed in many pulmonary and cardiac disorders or in premature births. The use of O_2 is however limited by its toxic effects (2,3). The by-products of O_2 metabolism (O_2^- and OH^-) cause O_2-mediated injury by interacting with cellular lipids, proteins, carbohydrates and nucleic acids. The antioxidant enzyme, e.g., superoxide dismutase (SOD) converts O_2^- into non-toxic H_2O_2. The therapeutic potential of SOD is limited *in vivo* due to its short half-life and rapid clearance by the kidneys (4). Furthermore, this enzyme is unable to cross cell membranes because it is a large molecule (5). Encapsulation of SOD within liposomes (6) would enhance its protective effect against intracellular O_2-mediated injury. Freeman et al. (7) suggested that both cell fusion and endocytosis play an important role in the intracellular delivery of liposome-entrapped SOD. Cationic liposomes made with stearylamine, cholesterol, and dipalmitoylphosphatidylcholine (DPPC) were found to be optimal for both entrapment efficiency and maximum binding by erythrocytes and endothelial cells (8). Using high-sensitivity differential scanning calorimetry (DSC), we found that there was no interaction between SOD and a neutral lipid such as the DPPC, but an interaction did occur with negatively charged dipalmitoylphosphatidylglycerol (DPPG) (9). To complement our DSC studies, we now report our Fourier transform infrared (FT-IR) spectroscopic studies on the conformational properties, thermal stability and temperature-induced folding-unfolding process of SOD before and after binding to DPPG. Elucidation of the physicochemical properties of SOD bound to lipid membranes may provide useful information on the mechanism of SOD action, and characteristics of SOD in lipid carriers.

EXPERIMENTAL: MATERIALS AND METHODS

Materials

Dipalmitoylphosphatidylglycerol (DPPG) (> 99.5 percent purity) was purchased from Avanti Polar Lipids Inc. (Alabaster, AL). The purity of this compound was tested by thin layer chromatography (TLC) with satisfaction and was used without further purification. SOD (bovine erythrocytes) was purchased from Calbiochem-Behring (La Jolla, CA). The purity of SOD had been tested by polyacrylamide gel electrophoresis (PAGE), as well as by sodium dodecyl sulfate polyacrylamide gel electrophoresis (SDS-PAGE) and fast-flow pressure liquid chromatography (FPLC: sperose 1030 column) (done by Calbiochem-Behring) with satisfaction (9).

Methods

Preparation of Protein-Lipid Complexes for FT-IR

SOD in D_2O (10.75 mg/ml if 50 μm spacer was used) is added to dry lipid films of a DPPG/D_2O concentration of 7.5 mg/ml (lipid-to-protein molar ratio of 26:1). The mixture is vortexed for 2 mins. Hydrogen-deuterium exchange is achieved by incubating the sample at 80°C for 3 hrs. This led to complete H/D exchange as judged by disappearance of bands near 1555 cm^{-1}. The reason for choosing such a high incubation temperature is that SOD is quite thermally stable with denaturation temperature at 100°C for the reduced form and 90°C for the

[1] Department of Pharmaceutics, University of Minnesota, Minneapolis, Minnesota 55455.
[2] Department of Pharmacy, Chia Nan Junior College of Pharmacy, 60 Erh-Jen Road, Sec. 1, Pao-An, Jen-Te Hsiang, Tainan Hsien, Taiwan, Republic of China.
[3] To whom correspondence should be addressed.

oxidized form. The protein solution is placed between demountable liquid flow cell with CaF_2 windows.

FT-IR Measurement

A Nicolet Magna-IR™ 550 spectrometer with a MCT detector is used to record the FT-IR spectra. The spectrometer is continuously purged with dry air for 30 mins to eliminate interference from water vapor. Then 128 scans are recorded at 2 cm^{-1} resolution. Spectral contributions from residual water are eliminated using a set of water vapor spectra measured under identical conditions (10). One precaution was taken, namely, the water spectra were recorded at the same temperature as that of the sample in order to take into account the temperature induced changes in the water spectrum. The subtraction factor was varied until the absorption region between 1700 and 1800 cm^{-1} was featureless, thereby avoiding artificial bands or water bands in the amide I and amide II regions of the protein spectrum. For temperature profile measurements, FT-IR spectra are collected continuously. The temperature of the model HT-32 heated demountable cell (Spectra-Tech) is controlled by a programmable temperature bath circulator (Neslab). The temperature is linearly increased at a rate of 0.5°C/min while recording approximately 128 interferograms per 1°C temperature change. For each temperature-dependent measurement, 3 independent determinations were performed. These results were reproducible, though they were not subjected to statistical analysis.

The spectra are Fourier deconvoluted using HWHH = 14.3–15.3 and a resolution enhancement factor of 2.4. It needs to be noted that the deconvolution routine may distort the original spectra, although the area under the bands are largely unaffected. For quantitative determination, deconvoluted spectra are then fitted using Grams/386™ program. Two assumptions are made here: 1) the deconvoluted spectra can fit well with *Gaussian* line shapes; 2) the molar absorptivities for the C=O bands of the different band components are alike.

RESULTS AND DISCUSSION

Effects of DPPG Binding on the Secondary Structure of SOD

Assignment of Component Bands to Elements of Specific Secondary Structure

The original FT-IR spectra of SOD in D_2O solution and complexed with DPPG at 28°C are compared. The peak position, relative area and band assignment for all the bands of amide I′ region of FSD spectra of SOD in solution and complexed with DPPG are summarized in Table 1 and will serve as a basis for the interpretation of structural changes of SOD in D_2O after DPPG binding for subsequent temperature experiments. The amide I′ band of the D_2O solution of SOD exhibits a maximum at 1646 cm^{-1}, together with some shoulders. The deconvoluted spectrum of SOD solution shows three dominant bands at 1654, 1646 and 1639cm^{-1}. Upon binding to DPPG, we observe changes in the amide I′ band contour from 1646 cm^{-1} to 1644 cm^{-1}. The deconvoluted spectrum of the DPPG-associated SOD shows three dominant bands at 1654, 1645 and 1639 cm^{-1}.

There are three major regions of band components; details for the band assignments are:

Table 1. Position of Amide I′ Component Bands, Relative Integrated Intensities, and Secondary Structure Assignments for SOD in D_2O Solution or in Complexes with DPPG at 28°C

	SOD[a] in D_2O		SOD/DPPG complex	
Structure[b]	cm^{-1}	% area	cm^{-1}	% area
β-Sheet (high frequency antiparallel)	1687	4.1	1687	4.0
β-Sheet (high frequency antiparallel)	1678	6.9	1678	5.9
Turn	1665	12.3	1668	8.0
			1661[c]	5.4
Helix-like hydrogen bonding pattern	1654	15.7	1654	15.7
Irregular	1646	18.6	1645	18.4
Twisted β-bend/3_{10}-helix	1640	9.2	1639	3.0
β-Sheet (low frequency antiparallel, main core)	1630	18.3	1631	27.0
β-Sheet (low frequency antiparallel, distorted)	1620	14.9	1619	12.6

[a] X-ray for SOD: 0% α-helix, 48% β-sheet, 18% right-handed turn, 14.9 left-handed turn, 19.1% irregular (23).

[b] The secondary structure band assignments were based on Byler and Susi, 1986 (13); Surewicz and Mantsch, 1988 (12).

[c] To fit the spectrum of SOD/DPPG in D2O, this additional component at 1661 was added to improve the agreement between the observed spectrum and the calculated spectrum. This addition helped to obtain the satisfactory fit of the corresponding spectra in the region between 1670 to 1640 cm^{-1}.

(1) The bands at 1620 and 1630 cm^{-1} are assigned to low-frequency components of antiparallel β-sheets with stronger hydrogen bonding. It is suggested by Fabian, et al., 1993 (10) that the band at 1630 is the main core β-sheet band, while the band at 1620 is the "distorted" β-type structures formed by peptide residues located at the end of β-sheets, by very short β-strands, or by the outer strands of β-sheets. Additional infrared-active components due to transition dipole coupling are expected in the region between 1675 and 1690 cm^{-1} for proteins containing antiparallel β-sheet structure (11). Therefore, the bands at 1678 and 1687 cm^{-1} are also assigned to antiparallel β-sheets with weaker hydrogen bonding. The four different β-components reflect different hydrogen bonding pattern between β-strands (12).

(2) The band at 1665 cm^{-1} is due to turns, which form a major structural elements of the three loops (12,13).

(3) The region between 1639 and 1660 is a large broad band. The Fourier self-deconvoluted spectra of SOD or SOD/DPPG show three major bands: 1640, 1646 and 1655 cm^{-1}. These three bands cannot be assigned unequivocally. The band at 1640 cm^{-1} is assigned to twisted β-bends, resulting from the change of the angle of rotation around N-C_α-bond and the angle around C_α-C′ for normal antiparallel β-sheets to some other degree. These bends are no longer the classical β-sheets and have weaker hydrogen bonding with higher frequency. This band could also be tentatively assigned to 3_{10}-helical turns (14). The band at 1646 cm^{-1} is

assigned to irregular structure (12,13), which may be due to the loop region or some other unordered structure. The band at 1654 cm^{-1} is assigned to the helix-like hydrogen bonding pattern, which may be due to a special kind of β-bend or turn and have the same absorption wavenumber as the normal α-helices. The special conformation of SOD with many antiparallel β-sheets and some other undefined structure may be one of the possible reasons for its high thermal stability.

Based on the above band assignments, the band fitting analysis of the deconvoluted spectra show that the secondary structure of SOD has some changes after DPPG binding at 28°C; the main difference is an increase in β-sheet content, this was calculated by 49.5% − 44.2% = 5.3% from Table 2. For Twisted β-bend/3_{10}-helix, this was calculated by 9.2% − 3.0% = 6.2% from Table 2. This suggests that after binding to DPPG, the content of β-sheet component of SOD increases at the expense of twisted β-bend/3_{10}-helix content.

Temperature-Dependent Conformational Changes of SOD

Figure 1 shows the Fourier self-deconvoluted infrared spectra of SOD recorded at different temperatures. The spectra measured between 28° and 77°C show three main changes: i) a gradual loss of β-sheet "distorted" structure (1620 cm^{-1} band); ii) loss of turns (1665 cm^{-1}) between 50 and 59°C and shifts to lower wavenumber (around 1662 cm^{-1}); iii) a larger shoulder at 1646 cm^{-1} at 50°C compared to 28°C. Based on the above observations, there seems to be an intermediate state around 50°C before the major conformational changes. Beginning at 80°C, changes are obtained in three temperature regions: 80°C, 92°C and 109°C. The temperature-induced conformational changes of SOD occur mostly in the region of 1640, 1646 and 1655 cm^{-1}, meaning that this region is unstable with higher molecular motion. The major structural changes occurred between 106° and 109°C. The spectra measured at temperature higher than 109°C have no further changes, indicating that the final stage of thermal denaturation has been reached. The temperature-induced spectral changes are quantified by curve-fitting techniques. Table 3 lists the peak positions and relative areas of the individual band components of the spectra at different temperatures. The relative intensity of the bands is retained between 28° and 77°C. Changes are observed at the following temperatures: (i) 80°C leads to the onset of protein unfolding (apo form of SOD). In comparison to the component band areas

Table 2. Secondary Structure Components of the Fourier Self-Deconvoluted FT-IR Spectra from SOD in D_2O Solution or in Complexes with DPPG at 28°C

	SOD in D_2O	SOD/DPPG complex
Structure	% area	% area
Turn	12.3	13.4
β-sheet	44.2	49.5
Helix-like hydrogen bonding pattern	15.7	15.7
Twisted β-bend/3_{10}-helix	9.2	3.0
Irregular	18.6	18.4

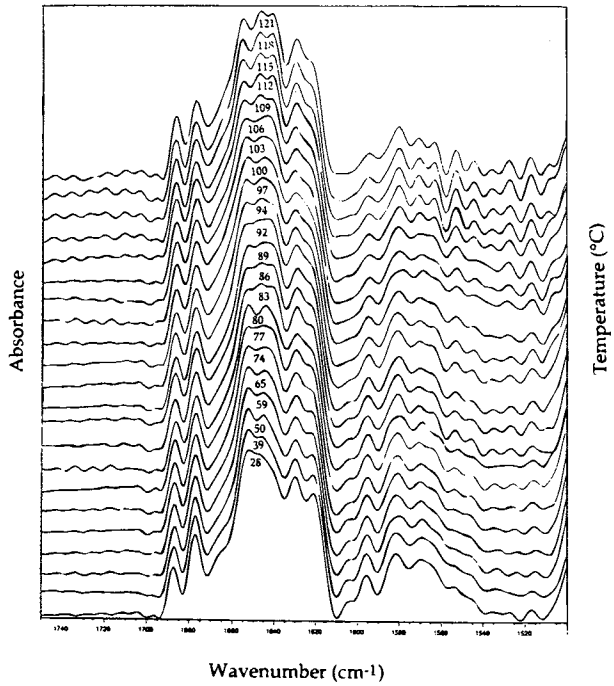

Fig. 1. Infrared spectra of SOD in D_2O solution recorded continuously at temperatures ranging from 28°–121°C. The temperature was linearly increased at a rate of 0.5°C/min. The spectra were Fourier self-deconvoluted using parameters provided under Methods.

at 77°C, the area for β-sheets decreases by 8%; the area for twisted β-bends decreases by 13% and the area for turns decreases by 6%; while the area for irregular structure increases by 29% (Table 3). However, there is no significant change in the area for helix-like hydrogen bonding pattern. This conclusion is made because the percentage change for helix-like hydrogen bonding pattern is only 2% (Table 3), well below the usual 5% error allowable in the literature. The above finding indicates that the unfolding of SOD starts within the regions of β-sheet, twisted β-bend and turn structures and changes into irregular structure in the first folding/unfolding state transition. (ii) 92°C leads to the onset of another protein unfolding (oxidized form of SOD). In comparison to the component band areas at 89°C, the area of the bands for turns decreases by 7%; while the area of the band for irregular structure increases by 7.5% (Table 3). This indicates that the unfolding of SOD starts within the regions of turn structures and irregular structures participate in the second folding/unfolding state transition. (iii) 109°C leads to the third onset of protein unfolding (reduced form of SOD). In comparison to the component band areas at 106°C, the area of the bands for helix-like hydrogen bonding pattern decreases by 10%, while the area of the band for irregular structure increases by 5% and the area for turns increases by 6% (Table 3). This indicates that the unfolding of SOD starts within the regions of helix-like hydrogen bonding pattern and irregular and turn structures participate in the third folding/unfolding state transition. However, we cannot rule out the possibility that the changes observed between 106° and 109°C is related to a drying-out process as water escapes from the cell at temperature higher than 100°C. (iv) higher than 109°C, the relative intensity of irregular structures remain high and that of helix-

Table 3. Peak Position (in cm^{-1}) and Relative Integrated Intensities (in %) of the Amide I′ Component Bands of SOD at Different Temperatures

Temp (°C)	28	39	50	59	65	74	77	80	83	86	89	92	94	97	100	103	106	109	112	115	118	121
V	1687	1687	1687	1687	1687	1687	1687	1687	1687	1687	1687	1687	1687	1687	1687	1687	1687	1687	1687	1687	1687	1687
A	4.1	4.2	4	3.8	3.8	3.8	3.9	4.0	4.0	4.1	4	4.3	4	4.2	4.8	4.6	4.9	4.6	4.6	4.7	4.7	4.8
V	1678	1678	1677	1678	1678	1678	1678	1678	1678	1678	1678	1678	1678	1678	1677	1678	1677	1678	1678	1678	1678	1678
A	6.9	6.5	7.1	5.9	5.4	5.2	6.1	5.5	6.0	5.9	5.5	6.8	5.6	7.6	8.6	7.8	8.8	7.9	7.8	7.7	7.6	7.5
V	1665	1664	1669					1667	1663	1663		1666		1670	1669	1670	1670	1671	1671	1672	1672	1671
A	12.3	14.7	5.3					10.9	17.2	18.8		12.5		4.4	3.6	4.4	2.3	1.6	2.6	0.9	1	1.2
V			1662	1662	1660	1659	1663	1656			1663		1664	1664	1663	1663	1665	1664	1664	1665	1664	1663
A			5.4	19.7	25.6	26.5	16.7	9.6			19.8		19.1	7.1	8.3	8.1	6.7	13.3	10.2	13.3	13.1	14.8
V	1654	1654	1654	1654	1654	1655	1654	1654	1655	1655	1654	1656	1654	1655	1655	1655	1656	1656	1657	1657	1657	1656
A	15.7	16.1	20	12.2	9.2	8.4	14.1	2.6	12.3	11.9	15	15	15.2	19.7	18.3	19	19.8	9.6	11.9	11.3	10.7	9.1
V	1646	1646	1646	1646	1646	1646	1647	1644	1648	1647	1647	1647	1646	1646	1646	1646	1646	1648	1648	1648	1648	1648
A	18.6	15.5	15.9	14.4	14.3	16.5	14	42.8	14.3	13.7	10.9	18.4	15.1	17.6	17.1	17.6	19.8	25	23.8	21.4	22.1	23.4
V	1639	1639	1639	1640	1640	1640	1640		1640	1641	1641	1640	1640	1640	1640	1640	1640	1640	1640	1640	1640	1640
A	9.2	9.4	10	10.1	9.1	5.7	12.7		15.7	13.6	12.5	11.3	8.4	6.8	9.5	6	6.4	7	8.5	11.6	10.7	9
V	1631	1630	1630	1630	1630	1630	1631	1629	1631	1631	1631	1630	1631	1631	1629	1631	1630	1630	1630	1630	1631	1630
A	18.3	19.8	18.9	22.1	20.3	24.1	19.4	13.2	16.7	20.1	21	21	21.9	23.5	23	23.7	23	21.8	23.3	19	20.3	20.7
V	1620	1620	1621	1620	1621	1620	1621	1621	1622	1621	1621	1621	1621	1621	1620	1621	1621	1621	1621	1621	1621	1621
A	14.9	13.9	13.8	11.9	12.2	9.9	13.1	11.5	13.8	11.9	11.4	10.8	10.7	9.1	6.7	8.9	8.2	9.3	7.8	10	10	9.6
β	44.2	44.3	43.8	43.7	41.8	43	42.5	34.2	40.6	42	41.9	42.8	42.1	44.4	43.1	44.9	44.9	43.6	43.4	41.5	42.5	42.5
h	15.7	16.1	19.7	12.2	9.2	8.4	14.1	12.2	12.3	11.9	15	15	15.2	19.7	18.3	19.0	19.8	9.6	11.9	11.3	10.7	9.1
i	18.6	15.5	15.9	14.4	14.3	16.5	14	42.8	14.3	13.7	10.9	18.4	15.1	17.8	17.1	17.6	19.8	25	23.6	21.4	22.1	23.4
t	12.3	14.7	10.7	19.7	25.6	26.5	16.7	10.9	17.2	18.8	19.8	12.5	19.1	11.5	11.9	12.5	9	14.9	12.8	14.2	14.1	16
tw	9.2	9.4	10	10.1	9.1	5.7	12.7		15.7	13.6	12.5	11.3	8.4	6.8	9.5	6	6.4	7	8.5	11.6	10.7	9

V: Peak positions are rounded to the nearest integer.
A: The band area as a fraction of the total amide I area set to 100%.
β: β-sheets.
h: helix-like hydrogen bonding pattern.
t: turns.
tw: twisted β-bends.
i: irregular structure.

like hydrogen bonding pattern remain low with small change in the band of β-sheets.

Temperature-Dependent Conformational Changes of SOD/DPPG

Figure 2 shows the Fourier self-deconvoluted infrared spectra of SOD/DPPG recorded at different temperatures. The temperature-induced spectral changes are quantified by curve-fitting techniques. Table 4 lists the peak positions and relative areas of the individual band components of the spectra at different temperatures. The spectral changes are not as obvious as those seen for SOD alone. There are three possible regions for folding/unfolding of SOD in DPPG (Figure 2): 77°C (apo form), 88°C (oxidized form), and 95°C (reduced form). The relative intensity of the bands is retained between 28° and 74°C. Changes are observed at the following temperatures: (i) 77°C leads to the onset of protein unfolding (apo form of SOD). In comparison to the component band areas at 74°C, the area for β-sheets decreases by 3% and the area for twisted β-bends decreases by 5.4%, while the area for helix-like hydrogen bonding pattern increases by 5%, while the area for irregular structure increases by 3.7% (Table 4). However, there is no significant change in the area for turns. This indicates that the unfolding of SOD starts within the regions of β-sheet and twisted β-bend structures and changes into helix-like hydrogen bonding pattern and irregular structure in the first folding/unfolding state transition. (ii) 88°C leads to the onset of another protein unfolding (oxidized form of SOD). In comparison to the component band areas at 85°C, the area of the bands for helix-like hydrogen bonding pattern decreases by 20%, while the area of the band for irregular structure increases by 6% , the area for turns increases by 9%, and the area for twisted β-bends increases by 4% (Table 4). This indicates that the unfolding of SOD starts within the regions of helix-like hydrogen bonding pattern structures, and irregular, turn and twisted β-bend structures participate in the second folding/unfolding state transition. (iii) 95°C leads to the third onset of protein unfolding (reduced form of SOD). In comparison to the component band areas at 91°C, the area of the bands for helix-like hydrogen bonding pattern decreases by 7%, while the area of the band for irregular structure increases by 8% (Table 4). This indicates that the unfolding of SOD starts within the regions of helix-like hydrogen bonding pattern and irregular structure participates in the third folding/unfolding state transition. (iv) higher than 95°C, the relative intensity of irregular structures remain high and that of helix-like hydrogen bonding pattern remain low with small change in the band of β-sheets.

An increase in the intensity of the amide I band around 1615–1620 cm^{-1} is frequently indicative of the formation of structure due to intermolecular hydrogen-bonded extended structures, formed upon aggregation of thermally unfolded proteins (15–17). The absence of this feature in our data indicates that the residual structure detected is not due to aggregation.

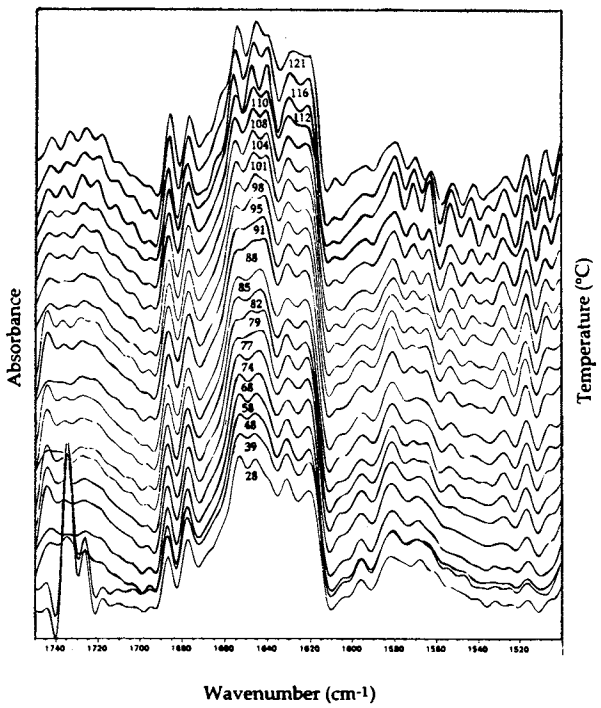

Fig. 2. Infrared spectra of SOD-DPPG complexes in D_2O solution recorded continuously at temperatures ranging from 28°–121°C, and Fourier self-deconvoluted as for SOD in Figure 1.

Absence of aggregation is also observed for RNase A (16,18,19), and RNase T_1 (20). The present study indicates that thermally denatured SOD in solution or complexed with DPPG retains its compact conformation with some residual secondary structure. This may be the reason for the high thermal stability of SOD.

Our studies suggest that binding of SOD to DPPG results in a marked decrease in the thermal stability of the protein, as indicated by the decrease of denaturation temperature of SOD.

Effects of SOD Binding on the Gel-to-Liquid Crystalline Phase Transition of DPPG

The Gel-to-Liquid Crystalline Phase Transition of Phospholipids

The carbon-hydrogen stretching vibrations of acyl chains observed by FT-IR have proven useful in characterizing the gel-to-liquid crystalline phase transition of phospholipids. The strongest bands for antisymmetric and symmetric methylene stretching modes appear near 2920 and 2850 cm^{-1}, respectively. The frequencies of these bands respond readily to temperature-induced changes of the *trans/gauche* ratio in acyl chains. The vibrational mode most suitable for following lipid structure changes in the presence of proteins is the CH_2 symmetric mode near 2850 cm−1. The advantage of monitoring this band is the lack of its overlapping with other vibrational bands, either from the terminal CH_3 groups or from the protein components.

Figure 3 (a and b) show the temperature dependence of FT-IR spectra of the 3100–2800 cm^{-1} region of DPPG in solution or complexed with SOD. Fig. 4 presents the frequency vs. temperature plots of the CH_2 symmetric vibration for DPPG

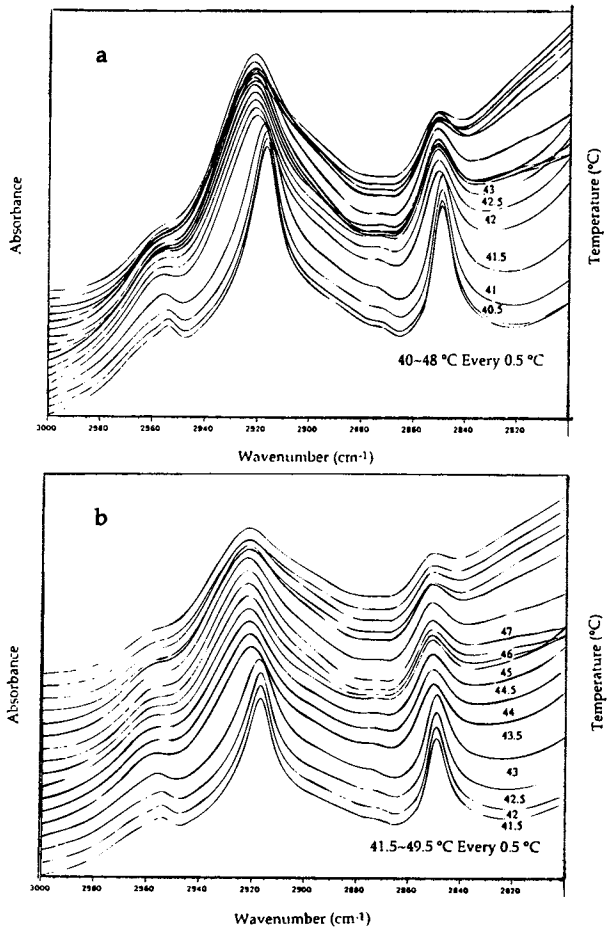

Fig. 3. (a) Temperature affected changes in infrared spectra of the CH_2 stretching mode (3100–2800 cm^{-1}) for DPPG in D_2O solution, showing a transition temperature at 42°C. (b) Temperature affected changes in infrared spectra of the CH_2 stretching mode for SOD-DPPG complexes in D_2O solution, showing a transition temperature at 43.5°C.

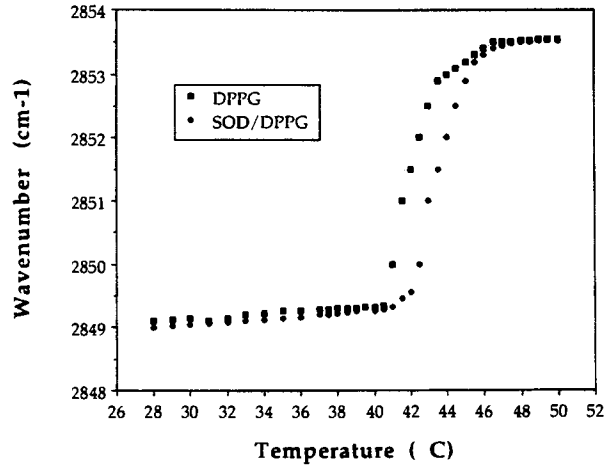

Fig. 4. A plot of wavenumbers vs. temperature (28°–50°C) in CH_2 symmetric stretching band in the infrared spectra of DPPG and SOD-DPPG complexes.

Table 4. Peak Position (in cm^{-1}) and Relative Integrated Intensities (in %) of the Amide I′ Component Bands of SOD/DPPG at Different Temperatures

Temp (°C)	28	39	48	58	68	74	77	79	82	85	88	91	95	98	101	104	108	110	112	116	121
V	1687	1687	1687	1687	1687	1687	1687	1687	1687	1687	1687	1687	1687	1687	1687	1687	1687	1687	1687	1687	1686
A	4.0	3.8	3.6	4.2	4.7	4.8	4.8	4.2	4.9	4.9	4.4	5.1	4.9	4.8	5	4.6	4.8	4.9	5.5	4.6	5.8
V	1678	1678	1678	1677	1678	1678	1678	1678	1678	1678	1678	1678	1678	1678	1678	1678	1677	1678	1678	1678	1677
A	5.9	4.7	4.2	6.0	5.9	6.8	6.4	4.8	6.8	6.8	5.4	6.8	6.5	6.4	5.8	3.9	3.7	5.9	6.2	7.8	6.3
V	1668	1663		1669	1664	1666	1666		1668	1668			1670	1669	1669	1667	1668	1671	1672	1671	1670
A	8	20.6		7.1	14.7	9.6	9.9		6.8	6.7			5.9	6.5	7.5	10.8	8.5	4.3	4.1	2.6	4.0
V	1661		1661	1661				1662			1665	1667	1663	1662	1663	1663	1663	1663	1664	1664	1662
A	5.4		24.7	6.3				8.9			15.7	9.7	5.6	7	5.1	1.8	3.4	7.5	8	10.2	10
V	1654	1653	1653	1654	1654	1656	1654	1656	1655	1654	1656	1656	1657	1655	1656	1656	1656	1656	1657	1657	1655
A	15.7	13.7	12.2	15.5	15.6	15.6	20.3	20.1	27.4	28.2	8.5	16.6	9.9	8.1	8.3	9.7	10.2	8.8	9.3	11.9	9.2
V	1645	1645	1645	1645	1644	1647	1643	1647	1642	1642	1647	1647	1647	1646	1647	1647	1648	1647	1648	1648	1647
A	18.4	14	13	19.4	20.1	20.8	24.5	19.2	21.6	20.1	26	20.3	28.2	27.5	26.2	26.9	27.1	24.2	23.7	23.8	23.7
V	1639	1640	1640	1639		1640		1640			1640	1640	1640	1640	1640	1640	1640	1640	1641	1640	1640
A	3	4.1	3.2	2.1		5.4		5.5			4.1	5.6	4	3.6	6.3	7.0	7.1	8.8	8.8	8.5	8.8
V	1631	1631	1631	1631	1629	1630	1629	1631	1630	1630	1631	1630	1630	1630	1630	1630	1630	1630	1630	1630	1628
A	27	27.4	28.4	28.7	28	25.7	23.3	26.4	20.5	21.7	24.9	24.9	24.8	27.1	26.4	25.4	25.8	27.2	25.5	23.3	26.1
V	1619	1619	1619	1620	1620	1620	1620	1620	1620	1620	1620	1620	1620	1620	1620	1620	1620	1620	1620	1621	1619
A	12.6	11.8	10.7	10.7	11.0	11.3	10.8	11	12	11.6	11.1	11	10.2	9	9.4	9.8	9.3	8.5	8.9	7.8	7.2
β	49.5	47.7	46.9	49.6	49.7	48.6	45.3	46.4	44.2	45.0	45.7	47.8	46.5	47.4	46.5	43.8	43.6	46.5	46.1	43.4	45.3
h	15.7	13.7	12.2	15.5	15.6	15.6	20.3	20.1	27.4	28.2	8.5	16.6	9.9	8.1	8.3	9.7	10.2	8.8	9.3	11.9	9.2
i	18.4	14	13	19.4	20.1	20.8	24.5	19.2	21.6	20.1	26	20.3	28.2	27.5	26.2	26.9	27.1	24.2	23.7	23.6	23.7
t	13.4	20.6	24.7	13.4	14.7	9.6	9.9	8.9	6.8	6.7	15.7	9.7	11.5	13.5	12.6	12.6	11.9	11.8	12.1	12.8	14
tw	3	4.1	3.2	2.1		5.4		5.5			4.1	5.6	4	3.6	6.3	7.0	7.1	8.8	8.8	8.5	8.8

V: Peak positions are rounded to the nearest integer.
A: The band area as a fraction of the total amide I area set to 100%.
β: β-sheets.
h: helix-like hydrogen bonding pattern.
t: turns.
tw: twisted β-bends.
i: irregular structure.

alone and for DPPG in the presence of SOD. The frequencies of the CH_2 symmetric band increases from about 2850cm^{-1} in the gel state to about 2853.5 cm^{-1} in the liquid crystalline state of DPPG at the transition temperature of 42°C. However, in the presence of SOD, the transition of DPPG shows a considerable broadening and the phase transition temperature increases to 43.5°C, meaning that the DPPG bilayers are stabilized by the SOD binding. This result is in complete agreement with our previous DSC studies (9), meaning that the DPPG bilayers are stabilized by the SOD binding.

Physical State of Acyl Chains at Temperature Below or Above the Transition Region

Data in Fig. 4 show that below the phase transition temperature, the frequencies of the CH_2 symmetric stretching vibrations are shifted to lower values when SOD is present. In contrast, no changes in frequency are observed when the temperature is above phase transition. Based on these findings, we conclude that SOD increases the ordering state of DPPG when it is in the gel state, but has no effect on the acyl chain conformation when DPPG is in the liquid crystalline state.

CONCLUSIONS

Due to its sensitivity, specificity and accuracy, FT-IR has emerged as an increasingly valuable tool to study the secondary structure of polypeptides and proteins in solution. Combined with computerized Fourier transform instrumentation and powerful mathematical band-narrowing techniques; namely Fourier self-deconvolution (FSD) and second derivative analysis, FT-IR spectroscopy permits quantitative determination of different secondary structural components of proteins (12,21). Specific information on the secondary structure provided by FT-IR has been obtained from the band changes in conformation-sensitive amide I band, which arises primarily from C=O stretching coupled to NH bending and CN stretching. From the band changes in the amide I′ region, the lipid-induced changes of protein secondary structure could be detected. We have presented an FT-IR spectroscopic study of the structure and stability of SOD in D_2O solution or complexed with DPPG. In addition, effects of lipid-binding on the temperature-induced folding-unfolding process of SOD has been determined using the relative changes in the characteristic band components for different secondary structural conformations.

Superoxide dismutase (SOD) is an important antioxidant enzyme with therapeutic potential against O_2-mediated injury. Our previous studies using high-sensitivity DSC (9) have shown that SOD binding to DPPG may be relevant to its ability to protect lipid membranes against oxygen-mediated injury. Using the FT-IR spectroscopy, the quantitative determination of the changes in the amide I band components of the Fourier self-deconvoluted spectra, the lipid-induced changes of SOD sec-

ondary structure could be detected as a function of temperature. We observe that the relative intensity of the SOD bands is retained from 28°C to 77°C. Beginning at 80°C, changes are observed at 80°, 92° and 109°C. The results suggest that SOD folding/unfolding transition involves mostly the relative changes within the regions of helix-like hydrogen bonding pattern, turn, twisted β-bend and irregular structures. When SOD is bound to DPPG, the conformational changes shift to lower temperatures, indicating a reduction of SOD thermal stability. In addition, upon binding to DPPG, there is an overall shift of the wavenumber to the right for 2 cm^{-1} at 28°C, indicating an increase in the accessibility of protein backbone amide groups to hydrogen-deuterium exchange. This suggests a lipid-mediated loosening and/or destabilization of the protein tertiary structure. The formation of less stable folding intermediates in an interfacial environment of phospholipid membranes may be related to a particular orientation of the protein during the reduction and oxidation process, or translocation across biological membranes, as recently reported by Endo et al., 1989 (22). These authors suggested that lipid-mediated conformational changes may account for one of the factors responsible for inducing and maintaining a loose, translocation-competent conformation of post-translationally translocated proteins. In addition, the gel to liquid crystalline phase transition temperature of DPPG increases from 42°C to 43.5°C, a result consistent with our findings by DSC. DPPG bilayer is stabilized by the presence of SOD. The finding of an increase in lipid transition temperature by the incorporation of SOD should also be useful for appropriate design of lipid carriers for SOD.

ACKNOWLEDGMENTS

We thank Dr. Henry H. Mantsch of National Research Council of Canada for his valuable advice and useful discussion on the analysis and interpretation of FT-IR results. The assistance of Ray Neff, Department of Chemical Engineering on the computer setup of FT-IR and temperature measurements is also appreciated. The partial financial support for Y.-L. Lo from the International Student Work Opportunity Program (ISWOP) of the University of Minnesota is also acknowledged.

REFERENCES

1. B. A. Freeman. Biology of Disease: Free Radicals and Tissue Injury. *Lab. Invest.* **47**:412–426 (1982).
2. R. R. Baker and B. A. Freeman. Exogenous Control of Pulmonary Antioxidant Defenses. In S. I. Said (ed.), *The Pulmonary Circulation and Acute Lung Injury,* Futura, New York, 1991, pp 473–496.
3. B. A. Freeman, P. C. Panus, S. Matalon, B. J. Buckley, and R. R. Baker. Oxidant Injury to the Alveolar Epithelium: Biochemical and Pharmacologic Studies. *Research Report* **54**:1–39 (1993).
4. A. Petkau, W. S. Chelack, K. Kelly, C. Barefoot, and L. Monasterski. Tissue Distribution of Bovine ^{125}I-superoxide Dismutase in Mice. *Res. Commun. Chem. Pathol. Pharmacol.* **15**:641–657 (1976).
5. A. M. Michelson. Clinical Use of Superoxide Dismutase and Possible Pharmacological Approaches. In A. P. Autor (ed.), *Pathology of Oxygen Radicals,* Academic Press, New York, 1982, pp. 277–302.
6. P. C. Panus and B. A. Freeman. Liposome-Entrapped Superoxide Dismutase: *in Vitro* and *in Vivo* Effects. In G. Gregoriadis (ed.), *Liposomes as Drug Carriers.,* Wiley, New York, 1988, pp 473–482.
7. B. A. Freeman, J. F. Turrens, Z. Mirza, J. D. Crapo, and S. L. Young. Modulation of Oxidant Lung Injury by Using Liposome-Entrapped Superoxide Dismutase and Catalase. *Fed. Proc.* **44**:2591–2595 (1985).
8. J. S. Beckman, R. L. Jr. Minor, and Freeman, B. A. Augmentation of Antioxidant Enzymes in Vascular Endothelium. *J. Free Radic. Biol. Med.* **2**:359–365 (1986).
9. Y.-L. Lo and Y. E. Rahman. Protein Location in Liposomes, A Lipid Carrier: A Prediction by Differential Scanning Calorimetry. *J. Pharm. Sci.* **84**:805–814 (1995).
10. H. Fabian, C. Schultz, D. Naumann, O. Landt, U. Hahn, and W. Saenger. Secondary Structure and Temperature-Induced Unfolding and Refolding of Ribonuclease T1 in Aqueous Solution. A Fourier Transform Infrared Spectroscopic Study. *J. Mol. Biol.* **232**:967–981 (1993).
11. S. Krimm and J. Bandekar. Vibrational Spectroscopy and Conformation of Peptides, Polypeptides and Proteins. *Advan. Protein. Chem.* **38**:181–364 (1986).
12. W. W. Surewicz and H. H. Mantsch. New Insight into Protein Secondary Structure from Resolution-Enhanced Infrared Spectra. *Biochim. Biophys. Acta* **952**:115–130 (1988).
13. D. M. Byler and H. Susi. Examination of the Secondary Structure on Proteins by Deconvoluted FTIR Spectra. *Biopolymers* **25**:469–487 (1986).
14. P. W. Holloway and H. H. Mantsch. Structure of Cytochrome b5 in Solution by Fourier-Transform Infrared Spectroscopy. *Biochem.* **28**:931–935 (1989).
15. A. Muga, H. H. Mantsch, and W. K. Surewicz. Membrane Binding Induces Destabilization of Cytochrome c Structure. *Biochem.* **30**:7219–7224 (1991).
16. S. Seshadri, K. A. Oberg, and A. L. Fink. Thermally Denatured Ribonuclease A Retains Secondary Structure As Shown by FTIR. *Biochem.* **33**:1351–1355 (1994).
17. A. Dong, S. J. Prestrelski, S. D. Allison, J. F. Carpenter. Infrared Spectroscopic Studies of Lyophilization- and Temperature-induced Protein Aggregation. *J. Pharm. Sci.* **84**:415–424 (1995).
18. A. H. Clark, D. H. P. Saunderson, and A. Suggett. Infrared and Laser-Raman Spectroscopic Studies of Thermally-Induced Globular Protein Gels. *J. Pept. Protein Res.* **17**:353–364 (1981).
19. T. Yamamoto and M. Tasumi. FT-IR Studies on Thermal Denaturation Processes of Ribonucleases A and S in H_2O and D_2O Solutions. *J. Mol. Struc.* **242**:235–244 (1991).
20. H. Fabian, C. Schultz, J. Backmann, U. Hahn, W. Saenger, H. H. Mantsch. Impact of Point Mutations on the Structure and Thermal Stability of Ribonuclease T1 in Aqueous Solution Probed by Fourier Transform Infrared Spectroscopy. *Biochem.* **33**:10725–10730 (1994).
21. J. L. Arrondo, R. A. Muga, J. Castresana, F. M. Goni. Quantitative Studies of the Structure of Proteins in Solution by Fourier-Transform Infrared Spectroscopy. *Prog. Biophy. Molecu. Biol.* **59**:23–56 (1993).
22. T. Endo, M. Eilers, and G. Schatz. Binding of a Tightly Folded Artificial Mitochondrial Precursor Protein to the Mitochondrial Outer Membrane Involves a Lipid-Mediated Conformational Change. *J. Biol. Chem.* **264**:2951–2956 (1989).
23. M. Levitt and J. Greer. Automatic Identification of Secondary Structure in Globular Proteins. *J. Mol. Biol.* **114**:181–239 (1977).